Available online at www.sciencedirect.com

SciVerse ScienceDirect

Ceramics International 39 (2013) 3035–3041

CERAMICS INTERNATIONAL

www.elsevier.com/locate/ceramint

Study on in-situ reaction synthesis and mechanical properties of Si_2N_2O ceramic

Xiangming Li[a,*], Litong Zhang[b], Xiaowei Yin[b]

[a]College of Water Resources and Architecture Engineering, Northwest Agriculture and Forestry University, Yangling, Shaanxi 712100, PR China
[b]National Key Laboratory of Thermostructure Composite Materials, Northwestern Polytechnical University, Xi'an, Shaanxi 710072, PR China

Received 2 September 2012; received in revised form 3 September 2012; accepted 21 September 2012
Available online 28 September 2012

Abstract

Si_2N_2O ceramics were fabricated using an in-situ reaction synthesis method by nitriding powder mixture of Si and SiO_2. The reaction mechanism in the Si–SiO_2–N_2 system was discussed by analyzing the variation of Gibbs free energy with temperature. As the sintering temperature rises from 1450 to 1700 °C, the Si_2N_2O phase increases with the Si_3N_4 phase decreasing and there is only Si_2N_2O with hardly any Si_3N_4 after sintering at 1700 °C, the volume shrinkage and mean pore size decrease respectively from 26.1% to 18.0% and from 0.4 to 0.04 μm, the porosity increases from 20.8% to 29.1%, and the Vickers hardness decreases from 5.6 to 4.5 GPa. After sintering at 1600 °C, Si_2N_2O ceramic possesses the highest flexural strength of 229 MPa and fracture toughness of 2.3 MPa $m^{1/2}$.

Keywords: Silicides; Microstructure; Mechanical properties; Structural applications

1. Introduction

Silicon oxynitride (Si_2N_2O) is the only compound in the SiO_2–Si_3N_4 system [1]. It has many good properties, such as good thermal shock resistance, high thermodynamic stability temperature about 1800 °C, excellent oxidation resistance in air up to 1600 °C and high flexural strength up to 1400 °C [2–9]. A thermodynamic calculation of the stability of Si_2N_2O indicates Si_2N_2O is more stable than Si_3N_4, so Si_2N_2O is a promising high-temperature structural material in place of Si_3N_4 in many fields. Si_2N_2O ceramics are usually fabricated by the in-situ reaction synthesis method, which is performed either through liquid phase by sintering an equimolar Si_3N_4 and SiO_2 mixture [9,10] or through gas phase by nitriding a mixture of Si and SiO_2 [11–13]. Si_2N_2O has a low diffusion coefficient and strongly covalent bond, requires high sintering temperature [14], so Si_2N_2O is difficult to be synthesized by reaction sintering an equimolar Si_3N_4 and SiO_2 mixture without the help of transition phase, and oxide additives are usually used to form a liquid phase with a eutectic melting point low enough to permit sintering without excessive dissociation [2,6–8,14]. When Si_2N_2O ceramic is fabricated by sintering equimolar Si_3N_4 and SiO_2 mixture by hot isostatic pressing method without adding any sintering aid, the maximum fraction of Si_2N_2O is 91.1% though the sintering temperature is high as 1900 °C. When sintering aid such as Li_2O, ZrO, Al_2O_3, MgO, Ln_2O_3 (where Ln = Yb, Er, Ce, Nb, Gd, Dy) is added, almost all Si_3N_4 and SiO_2 react with each other to produce Si_2N_2O, and Si_2N_2O ceramics possess better mechanical properties [2,6–9,14–17]. When Si_2N_2O ceramics are fabricated by nitriding a mixture of Si and SiO_2, the strong exothermic reaction propagates spontaneously through the reactant mixture, converting it into product [18], but the incomplete reaction of Si or SiO_2 decreases the properties of Si_2N_2O ceramic.

Si_2N_2O ceramics have been considered to be a high-temperature functional engineering material with a variety of potential applications, such as high-temperature electric insulator, nuclear-reactor moderator or reflector and solid electrolyte [11]. The functional applications of Si_2N_2O ceramics are seriously influenced by other phases, especially for Si, crystal SiO_2 and oxide additives, etc. When Si_2N_2O ceramics are fabricated by sintering a mixture of Si_3N_4 and SiO_2, the

*Corresponding author. Tel.: +86 29 87082902; fax: +86 29 87082901.
E-mail address: li_xiangming@yahoo.com (X. Li).

0272-8842/$ - see front matter © 2012 Elsevier Ltd and Techna Group S.r.l. All rights reserved.
http://dx.doi.org/10.1016/j.ceramint.2012.09.082

sintering aids acting as impurities disturb the material system inevitably. Fabricating Si_2N_2O ceramics by nitriding a powder mixture of Si and SiO_2 is more suitable for engineering applications due to its low-cost, but decreasing the residual Si or SiO_2 in Si_2N_2O ceramics is an urgent problem needing to be solved.

In the present work, Si_2N_2O ceramic is synthesized using a low-cost in-situ reaction synthesis method by nitriding powder mixture of Si and SiO_2. With the aim to decrease the residual Si and SiO_2 in Si_2N_2O ceramic, the reaction mechanism of possible reactions in the Si–SiO_2–N_2 system is discussed by analyzing the variation of Gibbs free energy with temperature. Using raw materials with very small particle size and defining suitable sintering temperature range according to thermodynamics analysis results, the effects of sintering temperature on the phase composition, porosity, pore size distribution, microstructure and mechanical properties of Si_2N_2O ceramic are investigated.

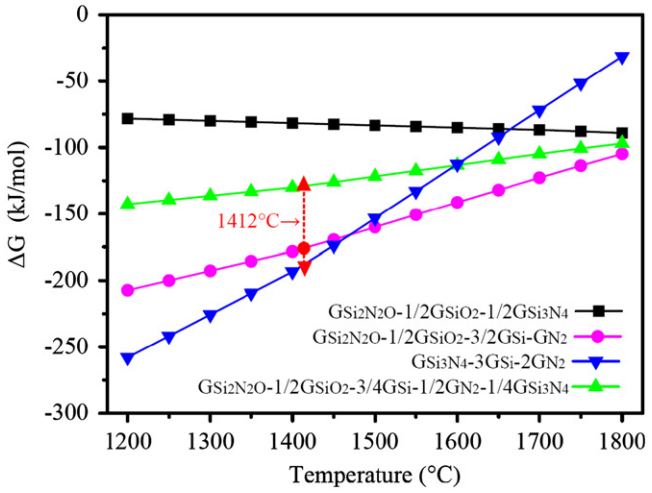

Fig. 1. Variation of Gibbs free energy of possible reactions in the Si–SiO_2–N_2 system as functions of temperature.

2. Thermodynamic considerations

Fig. 1 shows the variation of Gibbs free energy (ΔG) of possible reactions in the Si–SiO_2–N_2 system as functions of temperature. The ΔG given in Fig. 1 is calculated using the Factsage Thermodynamics Software (Thermfact/CRCT and GTT-Technologies, Canada and Germany). Two reaction synthesis methods are commonly used for fabricating Si_2N_2O according to following equations:

$$1/2SiO_2 + 1/2Si_3N_4 = Si_2N_2O \quad (1)$$

$$3/2Si + 1/2SiO_2 + N_2 = Si_2N_2O \quad (2)$$

As shown in Fig. 1, as the temperature rises from 1200 to 1800 °C, $\Delta G_T^0(1)$ decreases slightly from −78.3 to −89.1 kJ/mol, while $\Delta G_T^0(2)$ increases significantly from −207.3 to −104.8 kJ/mol. Therefore, the suitable synthesis temperature of Eq.(1) depends on the eutectic melting point, while lower temperature is good for Eq.(2) to take place theoretically without considering the kinetic factors. If Si_2N_2O is synthesized from Eq.(2) at lower temperature, lots of Si in the raw material could be nitrided into Si_3N_4 according to the following equation:

$$Si + 2N_2 = Si_3N_4 \quad (3)$$

As shown in Fig. 1, $\Delta G_T^0(3)$ increases quickly from −258.0 to −31.3 kJ/mol as the temperature rises from 1200 to 1800 °C. At temperature below 1450 °C $\Delta G_T^0(3)$ is lower than $\Delta G_T^0(2)$, which means Si is preferred to be nitrided into Si_3N_4. As the temperature rises to above 1450 °C, $\Delta G_T^0(3)$ becomes higher than $\Delta G_T^0(2)$, now the Si in the raw material reacts with SiO_2 and N_2 to produce Si_2N_2O. According to the above analysis, the sintering temperature should be higher than 1450 °C when fabricating Si_2N_2O ceramic from Eq.(2).

The melting point of Si is 1412 °C. If Si_2N_2O ceramic is fabricated from Eq.(2) directly at temperature above 1412 °C, the green body inevitably deforms due to the flow of liquid Si. For holding the shape well, the green body should be pre-nitrided at temperature below the melting point of Si for a short time. In order to fabricate pure Si_2N_2O ceramic, the best way for removing the produced Si_3N_4 is to make it react with SiO_2 to produce Si_2N_2O from Eq.(1). As is known, it is difficult for Si_3N_4 react with SiO_2 without the help of oxide additive which is in liquid phase at high temperature. However, when the green body is sintered at temperature above the melting point of Si, it is possible for Si_3N_4 to react with SiO_2 with the catalysis action of liquid Si, and the potential reaction is as follows:

$$3/4Si + 1/2SiO_2 + 1/4Si_3N_4 + 1/2N_2 = Si_2N_2O \quad (4)$$

As shown in Fig. 1, $\Delta G_T^0(4)$ increases from −142.8 to −97.0 kJ/mol as the temperature rises from 1200 to 1800 °C, and $\Delta G_T^0(4)$ is lower than $\Delta G_T^0(1)$, so it is feasible for Si_3N_4 react with SiO_2 from Eq.(4).

3. Experimental

3.1. Raw materials

Si powder was made by ball-milling the Si powder with particle size of 45 μm for 20 h using agate balls in an agate barrel. Observed by SEM, the mean particle size of Si powder after ball-milling is about 1.0 μm. Aerosil 200, an amorphous high-purity SiO_2 powder with very high specific area of $200 \pm 25\ m^2/g$ and mean particle size of 50 nm, is the initial powder used in the present work.

3.2. Fabrication process

According to Eq.(2), the Si powder was mixed with SiO_2 powder with a mole ratio of 3:1. The powder mixture was wet-milled in distilled water for 24 h, and then the powder slurry was freeze-dried and sieved through a 50 mesh screen. Green body with dimension of 5 mm × 10 mm × 70 mm

was fabricated by cold-pressing the powder mixture under 100 MPa. Finally, the green body was placed in an alumina crucible and sintered in 0.1 MPa fluid nitrogen gas by following heating and cooling steps: (a) increase the temperature to 1200 °C at a temperature rising rate of 5 °C/min, and then to 1400 °C at a temperature rising rate of 0.2 °C/min, (b) increase the temperature to 1400, 1450, 1500, 1550, 1600, 1650 and 1700 °C in order with the temperature rising rate of 5 °C/min and then hold for 2 h, (c) decrease the temperature to room-temperature at a cooling rate of 5 °C/min.

3.3. Characterization and tests

The open porosity and bulk density were measured by the Archimedes method. Phase analysis was conducted by X-ray diffraction (XRD), via a computer-controlled diffractometer (XRD, X'Pert Pro, Philips, the Netherlands). Microstructure was observed by scanning electron microscopy (SEM, JSM-6360LV, Electronics Co., Ltd., Japan). The pore size distribution was measured by a Mercury Porosimeter (Poremaster 33, Quantan Ltd, USA). The flexural strength was measured via the three-point bending test (CMT4204, Jiehu Instrument Co., Ltd. Shanghai, China) with a support distance of 30 mm and a loading speed of 0.5 mm/min. Five specimens with a dimension of 3 mm × 4 mm × 36 mm were tested to obtain the average strength. The fracture toughness was measured by the single edge notched beam (SENB) method. The edge notch with 2.5 mm length was made by a diamond cutting wheel and then finished with a razor blade and diamond paste. Five specimens with a dimension of $2.5 \times 5 \times 30\ mm^3$ were tested to obtain the average value. The Vickers hardness (Hv) was measured using a digital hardness tester (HBV-30 A, Huayin Experimental Apparatus Co, Shandong, China) with a pyramidal Vickers indenter. The specimens were indented with loads of 10 kg for 15 s and an average of eight indents was analyzed. Before mechanical property testing, all specimens were polished with 0.5 μm diamond paste as a final polishing step, then ultrasonically cleaned in acetone and air dried.

4. Results and discussion

4.1. Phase composition

The XRD pattern of Si_2N_2O ceramics sintered at different temperatures (Si_2N_2O-*n*, *n* means sintering temperature) is shown in Fig. 2. Besides unreacted Si, there are masses of α- and β-Si_3N_4 with little Si_2N_2O in Si_2N_2O-1400. Because of the restraining effect of nitrogen [19,20] and Si_3N_4 [21,22], most of SiO_2 in Si_2N_2O-1400 remains amorphous with little crystallized. Si_2N_2O-1450 possesses a primary phase of Si_2N_2O and secondary phase of α- and β-Si_3N_4. As is known, amorphous SiO_2 starts to crystallize when the temperature reaches to 1300 °C, and the nucleation of cristobalite is heterogeneous which starts from the surface of SiO_2 particles

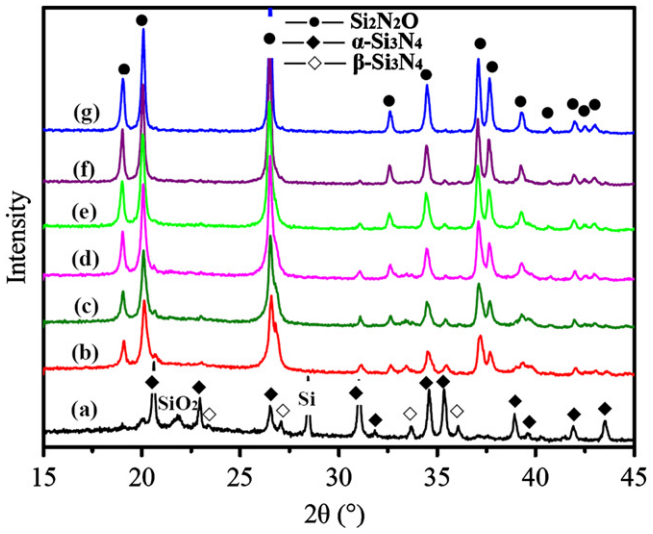

Fig. 2. XRD pattern of Si_2N_2O ceramics sintered at different temperatures.

[19,23,24], so when Si_2N_2O ceramic is fabricated by sintering at temperature above the melting point of Si, the SiO_2 particles in the green body may have chance to crystallize into cristobalite. However, liquid Si reacts with SiO_2 particles heterogeneously from the surface of SiO_2 particles to inside and the reaction speed is higher than the crystallization speed of SiO_2, so in the XRD pattern of Si_2N_2O-1450 there is no cristobalite detected and the amorphous phase is SiO_2 with a reason.

As known from Fig. 1, the $\Delta G_T^0(2)$ at 1400 °C is lower than that at 1450 °C, so the Si_2N_2O content in Si_2N_2O-1400 is theoretically more than that in Si_2N_2O-1450. $\Delta G_T^0(3)$ is lower than $\Delta G_T^0(2)$ when the temperature is below 1470 °C, which means Eq.(3) is easier to take place than Eq.(2) at 1450 °C. Actually, the Si_2N_2O content in Si_2N_2O-1450 is far higher than that in Si_2N_2O-1400. Fig. 3 gives the reaction model of the Si–SiO_2–N_2 system at temperatures below and above the melting point of Si respectively. When the green body is sintered at temperature below the melting point of Si (Fig. 3(a)), Eq.(2) could only take place at the contact area between Si and SiO_2 particles according to lattice diffusion, while Eq.(3) takes place rapidly to produce Si_3N_4 at the surface of Si particles. When the green body is sintered at temperature above the melting point of Si (Fig. 3(b)), the liquid Si surrounds the SiO_2 particles well, so Eqs.(2) and (4) take place easily, so there are lots of Si_2N_2O produced.

As the sintering temperature rises from 1450 to 1700 °C, $\Delta G_T^0(2)$ becomes far lower than $\Delta G_T^0(3)$, so Eq.(2) takes place even easier than Eq.(3). Besides, when the temperature rises to higher than 1650 °C, $\Delta G_T^0(4)$ also becomes lower than $\Delta G_T^0(3)$, leading to a faster decrease of Si_3N_4 in Si_2N_2O ceramic. As shown in Fig. 2, with temperature rising from 1450 to 1700 °C, Si_2N_2O ceramics increase in Si_2N_2O phase and decrease in Si_3N_4 phase, and there is only Si_2N_2O with hardly any Si_3N_4 in Si_2N_2O-1700.

4.2. Linear shrinkage and weight gain, density, porosity and pore size distribution

The linear shrinkage, weight gain, density and porosity of the Si_2N_2O ceramics sintered at different temperatures are listed in Table 1. Si_2N_2O-1400 is synthesized by solid-phase sintering, so the linear shrinkage of Si_2N_2O-1400 is only 1.7% in three directions. When the sintering temperature rises to above the melting point of Si, the volume shrinkage of Si_2N_2O ceramic gets large due to the liquid-phase sintering of Si_2N_2O ceramic. The production of Si_2N_2O has restraining effect on the shrinkage of Si_2N_2O ceramic, and the more Si_2N_2O produced, the more obvious the restraining effect shows. As listed in Table 1, due to the increase of Si_2N_2O production speed with temperature rising from 1450 to 1700 °C, the linear shrinkage of Si_2N_2O ceramic decreases from 9.6% to 6.4% in length (*L*) direction, from 9.0% to 6.3% in width (*W*) direction, and from 10.2% to 6.5% in thickness (*T*) direction. According to the linear shrinkage, Si_2N_2O ceramic decreases in volume shrinkage from 26.1% to 18.0%.

As the Si in the green body reacts completely with nitrogen and SiO_2 from Eq.(2) or with nitrogen from Eq.(3), the theoretical weight gain of Si_2N_2O ceramic is 38.9%. As shown in Table 1, the weight gain of Si_2N_2O-1400 is only 12.9% because of the incomplete reaction of Si, while the weight gain of Si_2N_2O-1450 is as high as 38.7% indicating an almost complete reaction of Si. At high temperature, SiO_2 and Si are volatile and the volatilization speed increases with temperature rising [25], so the Si_2N_2O ceramic decreases little in weight gain from 38.7% to 37.9% with temperature rising from 1450 to 1700 °C.

The density and porosity of Si_2N_2O ceramic are influenced together by the variation of volume shrinkage and weight gain. The density and porosity of Si_2N_2O-1400 are 1.41 g/cm^3 and 47.8% respectively. As the temperature rises to above the melting point of Si, Si_2N_2O ceramic increases significantly in density due to its increase in volume shrinkage and weight gain. However, as the temperature rises from 1450 to 1700 °C, the volume shrinkage and weight gain of Si_2N_2O ceramic decrease slowly, so the density of Si_2N_2O ceramic decreases from 2.22 to 1.99 g/cm^3 with the increase of porosity from 20.8% to 29.1%.

Fig. 4 shows the pore size distribution of Si_2N_2O ceramics sintered at different temperatures. As can be seen, the Si_2N_2O ceramics all show unimodal pore size distribution, and the pore size decreases with temperature rising. The pores in Si_2N_2O-1400 are of micro-size. As the

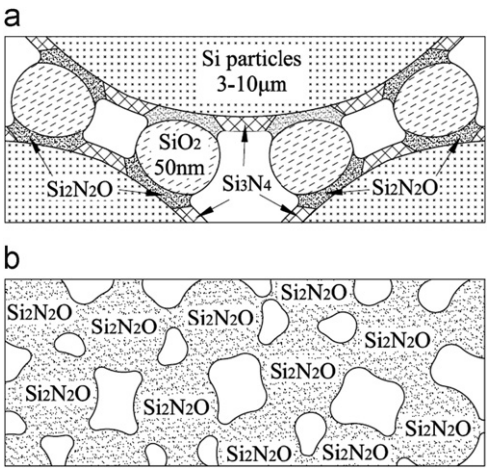

Fig. 3. Reaction model of the Si–SiO_2–N_2 system at temperatures (a) below and (b) above the melting point of Si.

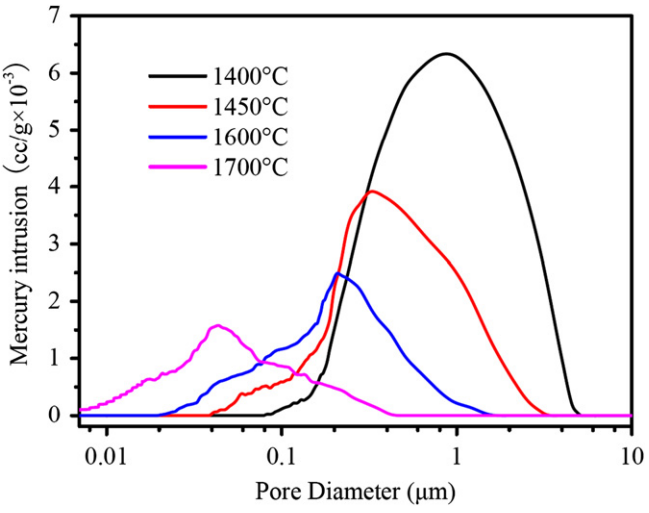

Fig. 4. Pore size distribution of Si_2N_2O ceramics sintered at different temperatures.

Table 1
Shrinkage, weight gain, density and porosity of Si_2N_2O ceramics sintered at different temperatures.

Temperature (°C)	Linear shrinkage (%)			Volume shrinkage (%)	Weight gain (%)	Density (g/cm^3)	Open porosity (%)
	L	*W*	*T*				
1400	1.7	1.7	1.7	5.0	13.5	1.41	47.8
1450	9.6	9.0	10.2	26.1	38.7	2.22	20.8
1500	8.6	8.1	9.1	23.6	38.6	2.15	23.4
1550	7.5	7.3	7.9	21.0	38.5	2.08	26.0
1600	6.9	6.8	7.1	19.4	38.3	2.03	27.6
1650	6.6	6.5	6.7	18.5	38.1	2.01	28.5
1700	6.4	6.3	6.5	18.0	37.9	1.99	29.1

temperature rises from 1450 to 1700 °C, the mean pore size of Si_2N_2O ceramic decreases from 0.4 to 0.04 μm.

4.3. Microstructure

Fig. 5 shows the micrographs at 10k-times magnification of Si_2N_2O ceramics sintered at different temperatures. During cold-pressing process, there are defects forms in the green body. Because of the small volume shrinkage of Si_2N_2O-1400, the defects are reserved and exist in the form of big pores in Si_2N_2O-1400 (Fig. 5(a)), and unreacted SiO_2 particles could be seen clearly. Due to the large volume shrinkage of Si_2N_2O-1450, the defects in Si_2N_2O-1450 (Fig. 5(b)) disappear, and the pores in Si_2N_2O-1450 are much smaller than that in Si_2N_2O-1400. As the temperature rises from 1450 to 1700 °C, Si_2N_2O ceramic increases in porosity from 20.8% to 29.1% and decreases in volume shrinkage from 26.1% to 18.0%, so the pores in Si_2N_2O ceramic theoretically increase. Seemingly, as can be seen by comparing Fig. 5(b)–(d), the pores in Si_2N_2O ceramic decrease on the contrary and the matrix gets denser with temperature rising.

Fig. 6 shows the micrographs at 50k-times magnification of Si_2N_2O ceramics sintered at different temperatures. In this magnification, it can be seen clearly that the matrix of Si_2N_2O ceramic is formed by stacking lots of 50 nm Si_2N_2O nano-particles, and there are lots of nano-pores among the nano-particles. By comparing Fig. 6(a)–(c), the pores in Si_2N_2O ceramic actually become more and bigger with temperature rising from 1450 to 1700 °C. The increase of the nano-pores makes the matrix of Si_2N_2O ceramic loose, and then influences the mechanical properties of Si_2N_2O ceramic.

4.4. Mechanical properties

From the above analysis, the phase composition, pore size distribution, porosity and microstructure of Si_2N_2O ceramic all vary with rising temperature, so the mechanical properties of Si_2N_2O ceramic are affected by these variations. Fig. 7 shows the flexural strength and fracture toughness of Si_2N_2O ceramics as functions of sintering temperature. Due to its high porosity and many big pores, Si_2N_2O-1400 possesses low flexural strength of 89 MPa and fracture toughness of 0.7 MPa $m^{1/2}$. Because of its low porosity and high Si_2N_2O content, Si_2N_2O-1450 possesses much higher flexural strength and fracture toughness than Si_2N_2O-1400. As the sintering temperature rises from 1450 to 1600 °C, the decrease of pore size makes the Si_2N_2O ceramic increase its flexural strength gradually from 183 to 229 MPa and fracture toughness from 1.9 to 2.3 MPa $m^{1/2}$. As the sintering temperature further rises to 1700 °C, because the matrix of Si_2N_2O ceramic gets loose, on the contrary Si_2N_2O ceramic decreases in flexural strength to 178 MPa and in fracture toughness to 1.9 MPa $m^{1/2}$.

Fig. 8 shows the Vickers hardness of Si_2N_2O ceramics as a function of sintering temperature. The Vickers hardness is affected both by phase composition and porosity. As to Si_2N_2O-1400, the Vickers hardness is only 2.4 GPa due to its high porosity. Si_2N_2O-1450 possesses high Vickers hardness due to its low porosity and high Si_2N_2O content. As the sintering temperature rises from 1450 to 1700 °C, the Si_2N_2O ceramic remains almost unchanged in phase composition but increases in porosity from 20.8% to 29.1%, so the Vickers hardness of Si_2N_2O ceramic decreases gradually from 5.6% to 4.5 GPa.

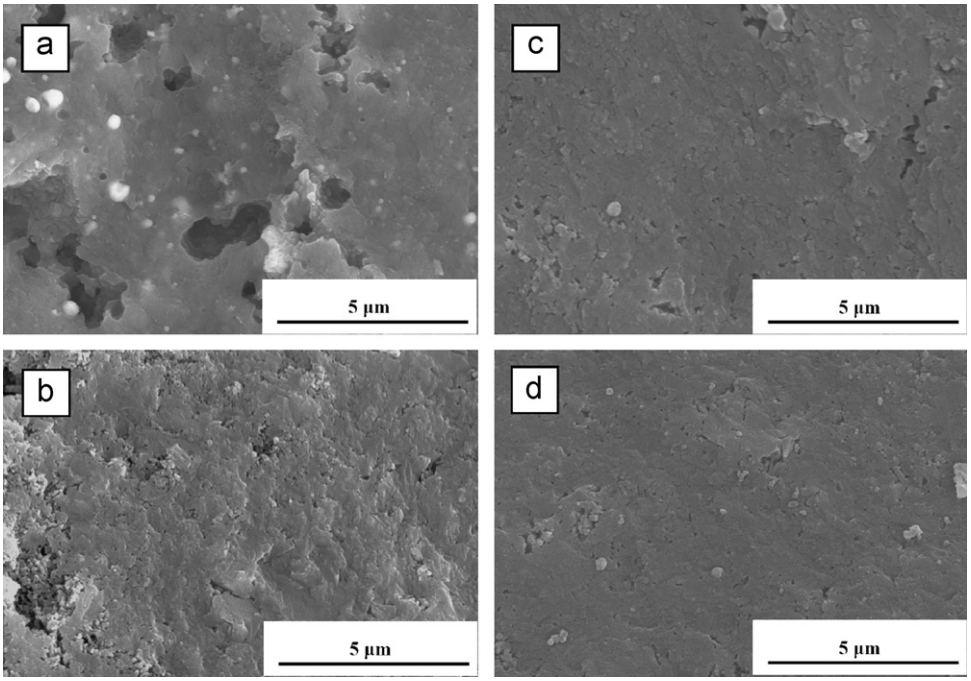

Fig. 5. Micrographs at 10k-times magnification of Si_2N_2O ceramics sintered at (a) 1400, (b) 1450, (c) 1600 and (d) 1700 °C.

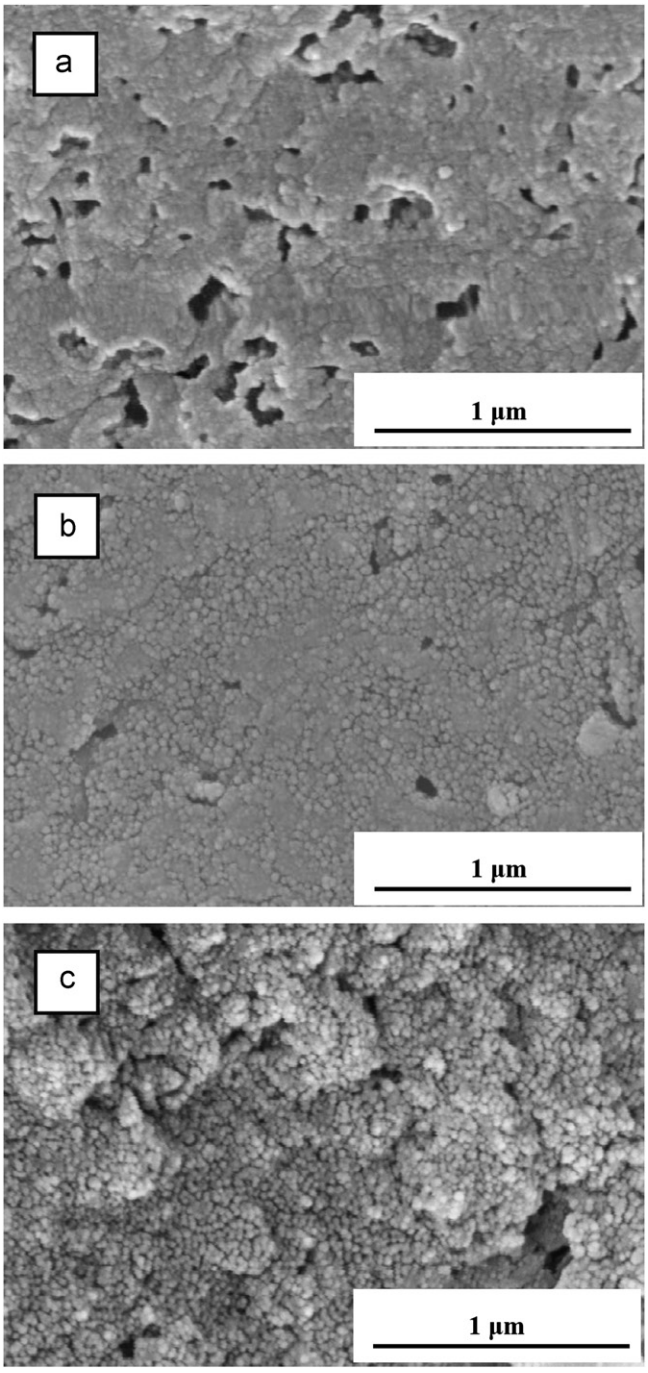

Fig. 6. Micrographs at 50k-times magnification of Si_2N_2O ceramics sintered at (a) 1450, (b) 1600 and (c) 1700 °C.

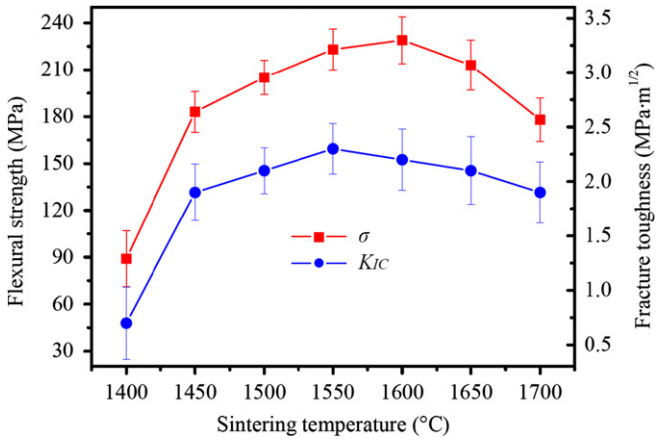

Fig. 7. Flexural strength and fracture toughness of Si_2N_2O ceramics as functions of sintering temperature.

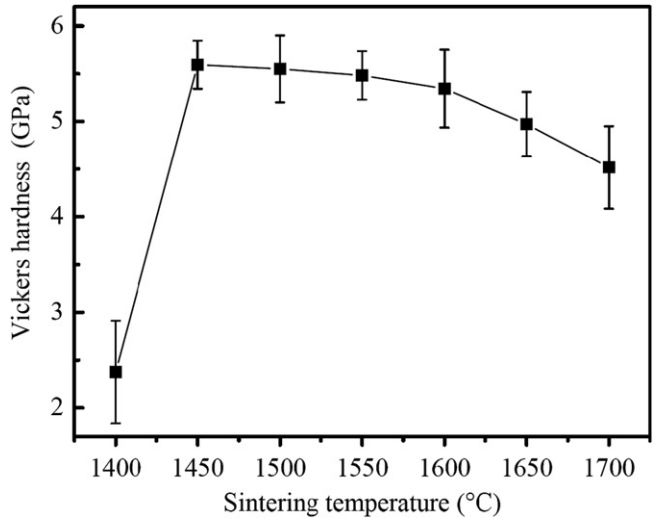

Fig. 8. Vickers hardness of Si_2N_2O ceramics as a function of sintering temperature.

5. Conclusions

Si_2N_2O ceramics were fabricated by an in-situ reaction synthesis method. The sintering temperature has a great effect on the phase composition, porosity, pore size distribution, microstructure and mechanical properties of Si_2N_2O ceramics.

1. The variation of phase composition with temperature coincides with the thermodynamics analyzing results of the $Si–SiO_2–N_2$ system. When the ceramic is sintered at temperature below the melting point of Si, Si_2N_2O is difficult to be produced. As the temperature rises to temperature above the melting point of Si, Si_2N_2O is produced easily and Si_3N_4 content decreases with temperature rising. There is only Si_2N_2O with hardly any Si_3N_4 in Si_2N_2O-1700.
2. At temperature above the melting point of Si, liquid-phase sintering makes Si_2N_2O ceramic shrink greatly, while the produced Si_2N_2O retards the volume shrinkage of Si_2N_2O ceramic. With the increase of Si_2N_2O production speed as the sintering temperature rises from 1450 to 1700 °C, the Si_2N_2O ceramic decreases gradually in volume shrinkage from 26.1% to 18.0% and in density from 2.22 to 1.99 g/cm^3.
3. After sintering at temperature above the melting point of Si, the defects in Si_2N_2O ceramic decrease significantly due to the large volume shrinkage, and there are hardly any big pores in Si_2N_2O ceramic. With temperature rising

from 1450 to 1700 °C, the nano-pores in Si_2N_2O ceramic increase greatly with big pores decreasing.

4. After sintering at temperature above the melting point of Si, the high Si_2N_2O content, small pore size and low porosity make Si_2N_2O ceramic possess good mechanical properties. Si_2N_2O-1600 possesses the highest flexural strength of 229 MPa and fracture toughness of 2.3 MPa $m^{1/2}$.

Acknowledgments

The authors gratefully acknowledge the financial support from the National Natural Science Foundation of China (No. 51209177) and the Basic Research Fund of Northwest Agriculture and Forestry University (No. Z109021203).

References

[1] M. Hillert, S. Jonsson, Thermodynamic calculation of the Si–Al–O–N system, Zeitschrift fur Metallkunde 83 (1992) 720–728.
[2] P. Rocabois, C. Chatillon, C. Bernard, Thermodynamics of the Si–O–N system: I. high-temperature study of the vaporization behavior of silicon nitride by mass spectrometry, Journal of the American Ceramic Society 79 (1996) 1361–1365.
[3] J.C. Bressiani, V. Izhevskyi, Ana.H.A. Bressiani, Development of the microstructure of the silicon nitride based ceramics, Materials Research 2 (1999) 165–172.
[4] B.T. Lee, J.H. Yoo, H.D. Kim, Effect of sintering additives on the nitridation behavior of reaction-bonded silicon nitride, Materials Science and Engineering A 333 (2002) 306–313.
[5] B.T. Lee, H.D. Kim, Effect of sintering additives on the nitridation behavior of reaction-bonded silicon nitride, Materials Science and Engineering A 364 (2004) 126–131.
[6] M. Ohashi, S. Kanzaki, H. Tabata, High-temperature flexural strength of hot-pressed silicon oxynitride ceramics, Journal of Materials Science Letters 7 (1988) 339–340.
[7] M. Ohashi, S. Kanzaki, H. Tabata, Processing, mechanical properties, and oxidation behavior of silicon oxynitride ceramics, Journal of the American Ceramic Society 74 (1991) 109–114.
[8] M. Ohashi, S. Kanzaki, H. Tabata, Effect of additives on some properties of silicon oxynitride ceramics, Journal of Materials Science 26 (1991) 2608–2614.
[9] Z.K. Huang, P. Greil, G. Petzow, Formation of silicon oxynitride from Si_3N_4 and SiO_2 in the presence of Al_2O_3, Ceramics International 10 (1984) 14–17.
[10] B. Bergman, H. Heping, The influence of different oxides on the formation of Si_2N_2O from SiO_2 and Si_3N_4, Journal of the European Ceramics Society 6 (1990) 3–8.
[11] R. Marchand, Y. Laurent, J. Guyader, P. L'Haridon, P. Verdier, Nitrides and oxynitrides: preparation, crystal chemistry and properties, Journal of the European Ceramics Society 8 (1991) 197–213.
[12] M. Billy, P. Boch, C. Dumazeau, J.C. Glandus, P. Goursat, Preparation and properties of silicon oxynitride-based ceramics, Ceramics International 7 (1981) 13–18.
[13] M. Mitomo, S. Ono, T. Asami, S.J.L. Kang, Effect of atmosphere on the reaction sintering of Si_2N_2O, Ceramics International 15 (1989) 345–350.
[14] Q.F. Tong, J.Y. Wang, Z.P. Li, Y.C. Zhou, Low-temperature synthesis densification and properties of Si_2N_2O with Li_2O additive, Journal of the European Ceramics Society 27 (2007) 4767–4772.
[15] W.Y. Ching, Electronic structure and bonding of all crystalline phase in the silica–yttria–silicon nitride phase equilibrium diagram, Journal of the American Ceramic Society 87 (2004) 1996–2013.
[16] Q.F. Tong, J.Y. Wang, Z.P. Li, Y.C. Zhou, Preparation and properties of Si_2N_2O/β-cristobalite composites, Journal of the European Ceramics Society 28 (2008) 1227–1234.
[17] R. Larker, Reaction sintering and properties of silicon oxynitride densified by hot isostatic pressing, Journal of the American Ceramic Society 75 (1992) 62–66.
[18] N. Pradeilles, M.C. Record, D. Granier, R.M. Marin-Ayral, Synthesis of b-SiAlON: a combined method using sol–gel and SHS processes, Ceramics International 34 (2008) 1189–1194.
[19] X.M. Li, X.W. Yin, L.T. Zhang, S.S. He, The devitrification kinetics of silica powder heat-treated in different conditions, Journal of Non-Crystalline Solids 354 (2008) 3254–3259.
[20] X.M. Li, X.W. Yin, L.T. Zhang, L.F. Cheng, Y.C. Qi, Mechanical and dielectric properties of porous Si_3N_4–SiO_2 composite ceramics, Materials Science and Engineering A 500 (2009) 63–69.
[21] C.M. Xu, S.W. Wang, X.X. Huang, J.K. Guo, G.H. Zhou, Crystallization and amorphization of cristobalite, Journal of Inorganic Materials 22 (2007) 577–582.
[22] C.M. Xu, S.W. Wang, X.X. Huang, J.K. Guo, Preparation of Si_3N_4/SiO_2 composites with pressureless sintering, Journal of Inorganic Materials 21 (2006) 935–938.
[23] F.E. Wagstaff, Crystallization kinetics of internally nucleated vitreous sillica, Journal of the American Ceramic Society 51 (1968) 449–452.
[24] F.E. Wagstaff, Crystallization and melting kinetics of cristobalite, Journal of the American Ceramic Society 52 (1969) 650–654.
[25] A. Daniel, Nitridation behaviour of silicon with clay and oxide additions: rate and phase development, Journal of the European Ceramics Society 17 (1997) 1613–1624.